Comparison of Hydride, Hydrogen Atom, and Proton-Coupled Electron Transfer Reactions

Sharon Hammes-Schiffer*[a]

A comparison of hydride, hydrogen atom, and proton-coupled electron transfer reactions is presented. Herein, hydride and hydrogen atom transfer refer to reactions in which the electrons and protons transfer between the same donor and acceptor, while proton-coupled electron transfer (PCET) refers to reactions in which the electrons and protons transfer between different centers. Within these definitions, hydride and hydrogen atom transfer reactions are typically electronically adiabatic, hence evolving on a single electronic surface. In contrast, PCET reactions are often electronically nonadiabatic since the electron transfers a longer distance through a proton transfer interface. For all three types of reactions, solute reorganization is important, particularly the hydrogen donor–acceptor mode. Solvent reorganization is critical for hydride transfer and PCET, which involve significant solute charge redistribution, but not for hydrogen atom transfer. Theoretical descriptions and simulation methodology for all three types of reactions are presented, as well as experimentally relevant applications to hydride transfer in enzymes and PCET in solution.

KEYWORDS:

electron transfer · hydrogen transfer · isotope effects · molecular dynamics · reaction mechanisms

1. Introduction

Hydride and hydrogen atom transfer reactions play a vital role in chemical and biological processes. At a fundamental level, these reactions may be described in terms of the transfer of protons and electrons. For example, a net hydride transfer involves the transfer of two electrons and one proton, and a net hydrogen atom transfer involves the transfer of one electron and one proton. In principle, both of these reactions are types of *proton-coupled electron transfer* (PCET) reactions, since they involve the coupled transfer of protons and electrons. For notational simplicity, however, in this Minireview the terms *hydride transfer* and *hydrogen atom transfer* refer to reactions in which the protons and electrons are transferred between the same donor and acceptor, while *PCET* refers to reactions involving the transfer of protons and electrons between different centers. These three situations are illustrated in Figure 1. Note that these definitions depend on only the initial and final states and are not rigorous due to the delocalized nature of electrons. Nevertheless, these definitions are implicitly used throughout the literature and are utilized in this Minireview for consistency and clarity.

These transfer reactions may be electronically adiabatic or nonadiabatic, where the term electronically adiabatic indicates that the electrons respond instantaneously to the nuclei (standard Born–Oppenheimer approximation). An electronically adiabatic reaction evolves on only the electronic ground state, while an electronically nonadiabatic reaction involves excited electronic states. The degree of electronic nonadiabaticity is determined by the energy difference between the ground and excited adiabatic electronic states during the reaction. If this energy difference is much larger than the thermal energy throughout the reaction, the reaction is electronically adiabatic, since the excited electronic states are not thermally accessible. If this energy difference becomes smaller than the thermal energy, however, the reaction is electronically nonadiabatic, since the excited electronic states are thermally accessible. In practice, the degree of electronic nonadiabaticity may be determined by calculating the coupling between the electronically diabatic reactant and product states, where smaller coupling leads to greater nonadiabaticity.[1, 2]

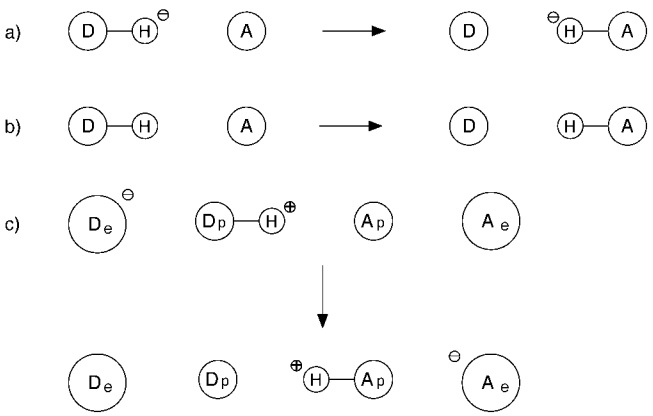

Figure 1. *a) Hydride transfer, b) hydrogen atom transfer, and c) PCET reactions. D and A are the donor and acceptor atoms, respectively.*

[a] *Prof. S. Hammes-Schiffer*
Department of Chemistry, 152 Davey Laboratory
Pennsylvania State University
University Park, PA 16802 (USA)
Fax: (+1) 814-863-5319
E-mail: shs@chem.psu.edu

Within these definitions, typically hydride and hydrogen atom transfer reactions are electronically adiabatic, while PCET reactions are electronically nonadiabatic. This difference may be understood in terms of the transfer distances. As discussed throughout the literature, single electron transfer reactions are electronically adiabatic for short distances and are electronically nonadiabatic for longer transfer distances. Hydride and hydrogen atom transfer reactions, in which the electron(s) and proton are transferred between the same donor and acceptor, are usually electronically adiabatic, since the electron transfer distance is relatively short, typically less than 3 Å. PCET reactions may be electronically adiabatic or nonadiabatic, and rate expressions have been derived for both of these limits.[51, 52] Typically, PCET reactions in which the electron donor and acceptor are well separated by the proton transfer interface (as depicted in Figure 1 c) are electronically nonadiabatic.

Nuclear quantum effects, such as zero point energy and hydrogen tunneling, have been shown to be important for these types of reactions. The hydrogen vibrational wavefunctions may be calculated for the transferring hydrogen nucleus moving in the potential due to the other nuclei along the reaction path. Figure 2 a depicts the two lowest-energy vibrational surfaces along a collective reaction coordinate for a symmetric hydrogen transfer reaction. Figure 2 b depicts the one-dimensional hydrogen potential energy curves and the corresponding energies of the hydrogen vibrational wavefunctions for three different values of the reaction coordinate. Note that the shape of the hydrogen potential energy curve changes along the reaction coordinate. For the equilibrium reactant configuration, the reactant well is lower in energy, and the lowest energy vibrational wavefunction is localized in this well. For the equilibrium product configuration, the product well is lower in energy, and the lowest energy vibrational wavefunction is localized in this well. At the avoided crossing, the two wells are degenerate, and the lowest energy vibrational wavefunction is delocalized between the two wells. The energy difference between the two lowest energy vibrational states at this point is the tunnel splitting, which determines the probability of hydrogen tunneling.

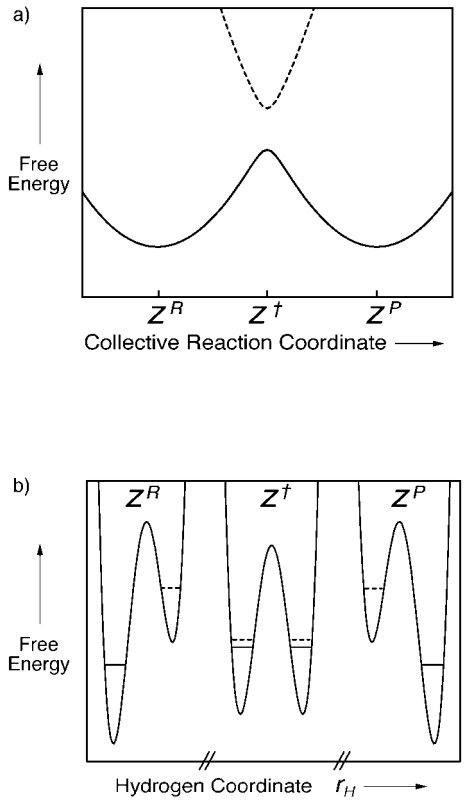

Figure 2. *a) Adiabatic vibrational free energy curves as functions of a collective reaction coordinate for a symmetric single hydride or hydrogen atom transfer reaction. b) Hydrogen potential energy curves as functions of the hydrogen coordinate r_H for three specific values of the reaction coordinate Z indicated in (a).*

In general, reactions may be vibrationally adiabatic or vibrationally nonadiabatic, where vibrationally adiabatic reactions remain in the ground vibrational state and vibrationally nonadiabatic reactions involve excited vibrational states. For hydrogen transfer reactions, the vibrationally adiabatic limit corresponds to the instantaneous response of the transferring hydrogen nucleus to the other nuclei. Although the splittings between the vibrational states associated with the motion of hydrogen nuclei in equilibrium configurations are typically much greater than the thermal energy, during the transfer of a hydrogen nucleus these splittings may become significantly smaller than the thermal energy (Figure 2 b). A hydrogen transfer reaction becomes more vibrationally nonadiabatic (the tunnel splitting decreases) as the barrier along the hydrogen coordinate becomes higher and wider. The height and width of the barrier are determined mainly by the donor – acceptor distance, where a larger donor – acceptor distance leads to a higher and wider barrier.

Hydride, hydrogen atom, and PCET reactions are driven by a combination of solvent fluctuations and intramolecular solute modes. Solvent reorganization is denoted *outer-sphere* and solute reorganization is denoted *inner-sphere* reorganization. Note that the distinction between solute and solvent is clear for reactions in solution but is not as straightforward for reactions in enzymes. The most critical solute mode for hydride transfer, hydrogen atom transfer, and PCET is the hydrogen donor – acceptor vibration, which determines the barrier along the hydrogen coordinate. For PCET reactions between metal complexes, the ligand – metal solute modes are also important. Solvent reorganization is important for reactions involving a substantial amount of solute charge redistribution. Thus, solvent reorganization is critical for hydride transfer and PCET, which involve significant solute charge redistribution, but not for hydrogen atom transfer. Note that the solvent reorganization energy reflects the difference between the charge distributions of the equilibrated initial and final states.

This Minireview outlines theoretical formulations and computational simulation methods for hydride, hydrogen atom, and PCET reactions. Section 2 centers on hydride and hydrogen atom transfer and describes a recent application to hydride transfer in the enzyme liver alcohol dehydrogenase. Section 3 centers on PCET and describes a recent application to PCET in iron biimidazoline complexes. The final Section presents an overview of future directions.

2. Hydride and Hydrogen Atom Transfer Reactions

A wide variety of theoretical and computational approaches for determining the rates of proton and hydride transfer reactions have been developed and applied to chemical and biological processes.[4–27] Both hydride and hydrogen atom reactions are usually electronically adiabatic, since the energy difference between the ground and excited electronic states is larger than the thermal energy throughout the reaction. As described above, hydride and hydrogen atom reactions may be vibrationally adiabatic or nonadiabatic. These reactions may be described in terms of a collective reaction coordinate comprised of solute and solvent modes. Solvent reorganization is important for hydride transfer due to the net transfer of a negative charge, while it is not important for hydrogen atom transfer reactions, which do not involve net charge transfer. Thus, the collective reaction coordinate includes significant contributions from both solute and solvent reorganization for hydride transfer, whereas it is dominated by solute modes for hydrogen atom transfer.

2.1. Theory

The overall rate expression for an electronically adiabatic reaction may be expressed according to Equation (1).

$$k = \kappa k_{TST} \quad (1)$$

The transition state theory (TST) rate constant k_{TST} is defined per Equation (2), where $\Delta G^{\ddagger}$ is the free energy barrier for the vibrationally adiabatic reaction and k_B is Boltzmann's constant.

$$k_{TST} = \frac{k_B T}{h} \exp\left[-\frac{\Delta G^{\ddagger}}{k_B T}\right] \quad (2)$$

The transmission coefficient κ accounts for recrossings of the dividing surface and includes vibrationally nonadiabatic effects.

An analytical expression for the electronically adiabatic free energy surface for proton or hydride transfer in solution is presented in ref. [28] as well as a prescription for obtaining the vibrationally adiabatic free energy barrier. This expression was derived within the context of dielectric continuum theory. Although it neglects solute reorganization, the effects of the solute modes are easily included. For example, the donor–acceptor vibration may be included by treating it quantum mechanically on the same level as the transferring hydrogen nucleus.

We have developed a hybrid approach for the real-time dynamic simulation of proton, hydride, and hydrogen atom transfer reactions in solution and enzymes. The electronic quantum effects are incorporated with an empirical valence bond (EVB) potential, and the nuclear quantum effects are included with a mixed quantum/classical method in which the transferring hydrogen nucleus is represented by a multidimensional vibrational wavefunction. A perturbation formula is utilized to incorporate the adiabatic nuclear quantum effects into the free energy profiles. The molecular dynamics with quantum transitions (MDQT) surface-hopping method is combined with a reactive flux approach to calculate the transmission coefficient and to investigate the real-time dynamics of reactive trajectories. This hybrid approach includes nuclear quantum effects, such as zero point energy, hydrogen tunneling, and nonadiabatic transitions, as well as the dynamics of the complete enzyme and solvent. These nuclear quantum effects are incorporated during the generation of the free energy profiles and dynamic trajectories rather than subsequently added as corrections. This approach allows the calculation of rates and kinetic isotope effects, as well as the analysis of real-time dynamic trajectories.

In the EVB approach, the ground state electronic wavefunction is expanded in a basis of VB states and the corresponding potential energy surface is the lowest eigenvalue of the Hamiltonian matrix in this basis set. For proton, hydride, and hydrogen transfer reactions, the minimal basis set consists of two VB states. For example, a hydride transfer reaction may be described in terms of the following two diabatic states, where D and A indicate the hydride donor and acceptor, respectively.

(*a*) $DH^- + A$

(*b*) $D + {}^-HA$

In VB state (*a*) the hydride ion is bonded to its donor, while in VB state (*b*) the hydride is bonded to its acceptor. The Hamiltonian matrix elements in this basis may be represented by standard molecular mechanical functional forms.

In our hybrid approach, the nuclear quantum effects of the transferring hydrogen are included by representing this nucleus as a multidimensional vibrational wavefunction. For this purpose, we use a mixed quantum/classical description of the nuclei, in which the transferring hydrogen nucleus with coordinate $\boldsymbol{r}$ is treated quantum mechanically, while the remaining nuclei with coordinates $\boldsymbol{R}$ are treated classically. The adiabatic vibrational wavefunctions for the transferring hydrogen can be calculated for fixed classical coordinates $\boldsymbol{R}$ by solving the time-independent Schrödinger Equation (3), where T_H is the kinetic energy of the transferring hydrogen and $V_{el0}(\boldsymbol{r},\boldsymbol{R})$ is the potential energy of the electronic ground state.

$$[T_H + V_{el0}(\boldsymbol{r},\boldsymbol{R})]\Phi_j(\boldsymbol{r};\boldsymbol{R}) = \varepsilon_j(\boldsymbol{R})\Phi_j(\boldsymbol{r};\boldsymbol{R}) \quad (3)$$

Equation (3) must be solved for each configuration of the classical nuclei during the generation of the free energy profiles and during the dynamic calculation of the transmission coefficient. To facilitate this calculation, we use the state-averaged Fourier grid Hamiltonian multiconfigurational self-consistent field (FGH-MCSCF) method to calculate multidimensional hydrogen vibrational wavefunctions.[29] Moreover, to further decrease the computational expense, we utilize a partial multidimensional grid generation method to decrease the number of potential energy calculations by avoiding these calculations for grid points with high potential energy.[30] This approach accurately describes ground- and excited-state hydrogen vibrational wavefunctions in a computationally practical manner.

As indicated by Equation (2), the calculation of the transition state theory rate constant requires the free energy barrier for the reaction. In our hybrid approach, the free energy barrier is determined from free energy profiles that depend on a collective

reaction coordinate analogous to the reaction coordinate in Marcus theory for electron transfer.[31–34] This collective reaction coordinate may be defined per Equation (4), where $\langle \ldots \rangle_{\boldsymbol{r}}$ indicates integration over the quantum coordinate $\boldsymbol{r}$, $\Phi_0(\boldsymbol{r};\boldsymbol{R})$ is the groundstate vibrational wavefunction, and V_{11} and V_{22} are the diagonal matrix elements of the EVB Hamiltonian.

$$\Lambda^{(q)}(\boldsymbol{R}) = \langle \Phi_0(\boldsymbol{r};\boldsymbol{R}) \,|\, V_{22}(\boldsymbol{r},\boldsymbol{R}) - V_{11}(\boldsymbol{r},\boldsymbol{R}) \,|\, \Phi_0(\boldsymbol{r};\boldsymbol{R}) \rangle_{\boldsymbol{r}} \quad (4)$$

A mapping or umbrella potential is used to drive the reaction over the barrier for infrequent events. Equation (5) is an example of a mapping potential.

$$V_{\mathrm{map}}(\boldsymbol{r},\boldsymbol{R};\lambda) = (1-\lambda)V_{11}(\boldsymbol{r},\boldsymbol{R}) + \lambda V_{22}(\boldsymbol{r},\boldsymbol{R}) \quad (5)$$

Variation of the parameter λ from zero to unity drives the reaction from the reactant VB state (*a*) to the product VB state (*b*). The adiabatic quantum free energy profiles are calculated from molecular dynamics simulations with a combination of perturbation formulas and thermodynamic integration.[35] These free energy profiles include the vibrationally adiabatic nuclear quantum effects by representing the transferring hydrogen nucleus as a multidimensional vibrational wavefunction.

In dynamic systems, the environment may cause trajectories to recross the dividing surface. The transition state theory rate constant k_{TST}, defined in Equation (2), is based on the assumption that each trajectory passes through the dividing surface only one time. The "exact" rate constant k, as given in Equation (1), accounts for recrossings of the dividing surface through the transmission coefficient κ. In classical molecular dynamics simulations, κ may be calculated by means of reactive flux methods for infrequent events.[36–39] In this approach, κ is calculated as the flux-weighted average of a quantity ξ for a canonical ensemble of classical molecular dynamics trajectories started at the dividing surface and integrated backward and forward in time. The quantity ξ corrects for multiple crossings of the dividing surface, so that all trajectories that originate as reactants and end as products are counted only once, no matter how many times they cross the dividing surface, and all trajectories that go from reactants to reactants, products to products, or products to reactants are not counted at all. In particular, $\xi = 1/\alpha$ for trajectories that have α forward crossings and $\alpha - 1$ backward crossings of the dividing surface, and $\xi = 0$ otherwise.

In our hybrid approach, nuclear quantum dynamic effects are incorporated in the calculation of κ by a combination of the MDQT mixed quantum/classical method[3, 40, 41] and the reactive flux method for infrequent events.[35] The fundamental principle of MDQT is that an ensemble of trajectories is propagated, and each trajectory moves classically on a single adiabatic surface except for instantaneous transitions among the adiabatic vibrational states. The adiabatic wavefunctions $\Phi_n(\boldsymbol{r};\boldsymbol{R})$ with energies $\varepsilon_n(\boldsymbol{R})$ are calculated at each classical molecular dynamics time step by solving Equation (3).[29] The classical nuclei evolve according to Newton's equations of motion with the effective potential $\varepsilon_k(\boldsymbol{R})$, where k denotes the occupied adiabatic state. The time-dependent wavefunction describing the quantum nuclei is expanded in a basis of the adiabatic states according to Equation (6).

$$\Psi(\boldsymbol{r},\boldsymbol{R},t) = \sum_{j=0}^{N_{\mathrm{ad}}-1} C_j(t)\Phi_j(\boldsymbol{r};\boldsymbol{R}) \quad (6)$$

The quantum amplitudes $C_j(t)$ are calculated by integration of the time-dependent Schrödinger equation simultaneously with the classical equations of motion. At each time step, Tully's "fewest switches" algorithm[40] is invoked to determine if a quantum transition to another adiabatic state should occur. This algorithm correctly apportions trajectories among the adiabatic states according to the quantum probabilities $|C_j(t)|^2$ with the minimum required number of quantum transitions (neglecting difficulties with classically forbidden transitions).

The use of the standard classical reactive flux approach in conjunction with MDQT is problematic, since the probability of nonadiabatic transitions depends on the quantum amplitudes, which depend on the history of the trajectory. Thus, trajectories started at the dividing surface cannot be propagated backward in time with the MDQT method. (Backward propagation requires knowledge of the quantum amplitudes at the dividing surface, which are unavailable.) In order to surmount this difficulty, we use the method developed by Hammes-Schiffer and Tully[42] to simulate infrequent events in reactions which evolve on multiple potential energy surfaces.[42] In this approach, trajectories are started at the dividing surface and propagated backward in time with a fictitious surface-hopping algorithm that does not depend on the quantum amplitudes. The trajectory is then propagated forward in time, retracing the exact same trajectory, integrating the quantum amplitudes and calculating the probabilities for nonadiabatic transitions for each time step using the true surface-hopping algorithm. Each trajectory is assigned a weighting to ensure that the overall results are identitical to those that would have been obtained with the true surface-hopping algorithm.

2.2. Application

The hybrid approach described in Section 2.1 has been applied to hydride transfer in the enzyme liver alcohol dehydrogenase (LADH).[35, 43] LADH catalyzes the reversible oxidation of alcohols to aldehydes or ketones by the coenzyme nicotinamide dinucleotide (NAD^+). The mechanism involves the transfer of a hydride between two carbon atoms, as depicted in Figure 3. This

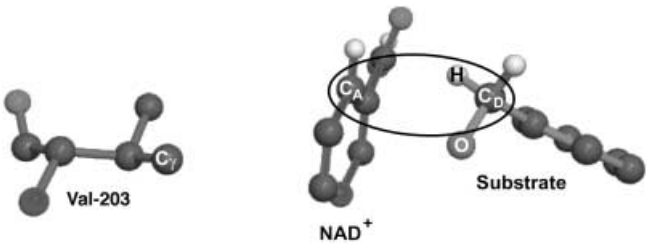

Figure 3. *Hydride transfer reaction from C_D of the benzyl alkoxide substrate to C_A of the cofactor NAD^+ in the enzyme LADH. The neighboring residue Val-203 is also depicted.*

enzyme was chosen as a prototype to test this method due to its biochemical importance, the availability of a high-resolution crystal structure,[44, 45] and experimental kinetic isotope effect experiments indicating significant hydrogen tunneling.[46–48]

We developed an EVB potential for this system based on the GROMOS forcefield.[49] The system used in these calculations contains the protein dimer, two NAD^+ cofactors, two benzyl alkoxide substrates, and 22682 water molecules, resulting in a total of 75140 atoms. Morse potentials were included for the bonds between the transferring hydride and the donor and acceptor carbon atoms. The two parameters corresponding to the relative energies of the two diagonal elements and the off-diagonal element of the EVB Hamiltonian were adjusted to reproduce the experimental free energies of activation and reaction.

The calculated free energy profiles for hydrogen, deuterium, and tritium transfer are shown in Figure 4. The transmission coefficients were found to be nearly unity, suggesting that nonequilibrium dynamic effects, such as barrier recrossings, are not dominant for this reaction. Furthermore, nonadiabatic effects were not significant for this system. The deuterium and tritium kinetic isotope effects calculated with this hybrid approach are in agreement with experimental data.[48]

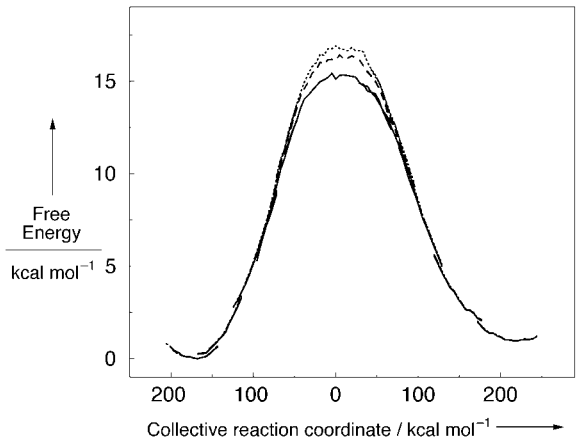

Figure 4. *Free energy profiles for hydrogen (——), deuterium (- - - -), and tritium (····) transfer in LADH along the collective reaction coordinate. Data reproduced with permission from ref. [37].*

An analysis of the geometrical properties in these simulations provided insight into the relation between specific enzyme motions and the enzyme activity. Moreover, this approach distinguishes between enzyme motions which influence the nonequilibrium dynamic barrier recrossing and enzyme motions which influence the equilibrium between the transition state and the reactant. The donor – acceptor distance, the catalytic zinc – substrate oxygen distance, and the coenzyme (NAD^+/NADH) ring angles were found to strongly impact the activation free energy barrier. For example, the evolution of the average donor – acceptor distance along the collective reaction coordinate is depicted in Figure 5 a. This distance decreases to approximately 2.7 Å in the transition state region, as expected from previous electronic structure calculations for model systems. The donor – acceptor distance and one of the coenzyme ring angles were found to impact the transmission coefficient as they were correlated to the degree of dynamic barrier recrossing.

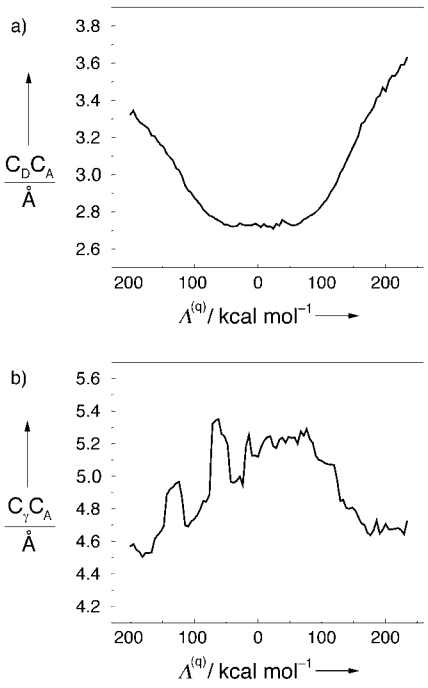

Figure 5. *Equilibrium averages of a) the donor – acceptor distance and b) the Val-203 C_γ – acceptor distance along the collective reaction coordinate. Data reproduced with permission from ref. [37].*

These simulations also provided insight into the impact of mutations in LADH. In particular, Klinman and co-workers observed experimentally that the rate of hydride transfer decreases when Val-203 is replaced by the smaller residue alanine.[50] Our simulations indicated that the distance between Val-203 and the reactive center significantly impacts the activation free energy but is uncorrelated to the degree of barrier recrossing. The evolution of the average distance between C_γ of Val-203 and the acceptor carbon along the reaction coordinate is depicted in Figure 5 b. These simulations suggest that the motion of Val-203 directs the acceptor carbon atom toward the donor carbon atom through steric interactions involving the C_γ atoms of Val-203. When Val-203 is replaced with alanine, the C_γ atoms of Val-203 are no longer available for these steric interactions, which leads to a decrease in the rate of hydride transfer. This application illustrates the power of this approach in the elucidation of enzyme mechanisms.

3. Proton-Coupled Electron Transfer Reactions

As mentioned in the introduction, PCET reactions may be electronically adiabatic or nonadiabatic. This Section focusses on PCET reactions in which the electron is transferred through a proton transfer interface. These PCET reactions are typically electronically nonadiabatic due to weak coupling between the reactant and product electronic states. As for hydrogen atom and hydride transfer reactions, the nuclear quantum effects of

the transferring hydrogen are important for PCET reactions. Solute modes, including the donor – acceptor and metal – ligand vibrations, play a significant role during the reaction. In addition, since PCET reactions involve substantial solute charge redistribution, solvent reorganization is important for these reactions in polar solvents. Recently PCET reactions have been studied with a range of theoretical methods.[28, 51–64] Note that these formulations are also applicable to general PCET reactions in which the transferring proton is not directly between the electron donor and acceptor.

3.1. Theory

The theoretical description of the most basic PCET reaction involving the transfer of one electron and one proton requires four diabatic states:[59]

(*1a*) $D_e^{-}-{}^{+}D_pH\cdots A_p-A_e$
(*1b*) $D_e^{-}-D_p\cdots HA_p^{+}-A_e$
(*2a*) $D_e-{}^{+}D_pH\cdots A_p-A_e^{-}$
(*2b*) $D_e-D_p\cdots HA_p^{+}-A_e^{-}$.

In this notation, *a* and *b* indicate the proton transfer (PT) state, and *1* and *2* indicate the electron transfer (ET) state. If the initial state is *1a*, a transition to *1b* corresponds to PT, a transition to *2a* corresponds to ET, and a transition to *2b* corresponds to EPT (in which both the electron and the proton are transferred).

Soudackov and Hammes-Schiffer have derived a rate expression for electronically nonadiabatic PCET reactions.[51] In this derivation, the Golden Rule is used to calculate the rate of transitions between two sets of mixed electronic/vibrational free energy surfaces corresponding to the two diabatic states for ET. The rate expression is given in Equation (7), where Σ_μ and Σ_ν indicate a sum over vibrational states associated with ET diabatic state *1* and *2*, respectively, and P_μ^{I} is the Boltzmann factor for state $\mathrm{I}\mu$.

$$k = \frac{2\pi}{\hbar}\sum_{\mu} P_{\mu}^{\mathrm{I}} \sum_{\nu} V_{\mu\nu}^{2} (4\pi\lambda_{\mu\nu} k_{\mathrm{B}} T)^{-1/2} \exp\left\{ - \frac{(\Delta G_{\mu\nu}^{0} + \lambda_{\mu\nu})^{2}}{4\lambda_{\mu\nu} k_{\mathrm{B}} T} \right\} \quad (7)$$

The free energy difference is defined in Equation (8) in terms of free energy surfaces $\varepsilon_\mu^{\mathrm{I}}$ and $\varepsilon_\nu^{\mathrm{II}}$ with minima $\vec{z}^{\mathrm{I}\mu}$ and $\vec{z}^{\mathrm{II}\nu}$, respectively.

$$\Delta G_{\mu\nu}^{0} = \varepsilon_{\nu}^{\mathrm{II}}(\vec{z}^{\mathrm{II}\nu}) - \varepsilon_{\mu}^{\mathrm{I}}(\vec{z}^{\mathrm{I}\mu}) \quad (8)$$

The total reorganization energy is expressed in Equation (9) as the sum of the outer-sphere and inner-sphere contributions in the classical limit (when the inner-sphere modes correspond to energies smaller than the thermal energy).

$$\lambda_{\mu\nu} = (\lambda_0)_{\mu\nu} + \lambda_i \quad (9)$$

The outer-sphere reorganization energy is defined per Equation (10) and the inner-sphere reorganization energy λ_i may be calculated with a standard harmonic approximation based on the experimentally or theoretically determined force constants and bond length changes for the relevant vibrational modes.[65]

$$(\lambda_0)_{\mu\nu} = \varepsilon_{\mu}^{\mathrm{I}}(\vec{z}^{\mathrm{II}\nu}) - \varepsilon_{\mu}^{\mathrm{I}}(\vec{z}^{\mathrm{I}\mu}) = \varepsilon_{\nu}^{\mathrm{II}}(\vec{z}^{\mathrm{I}\mu}) - \varepsilon_{\nu}^{\mathrm{II}}(\vec{z}^{\mathrm{II}\nu}) \quad (10)$$

The coupling $V_{\mu\nu}$ is averaged over the reactant and product proton vibrational wavefunctions $\mathrm{I}\mu$ and $\mathrm{II}\nu$. In the evaluation of $V_{\mu\nu}$, the overlap of the reactant and product proton vibrational wavefunctions plays a role similar to that of the Franck – Condon overlap factor in theories including quantum mechanical inner-sphere modes for single electron transfer. A more general rate expression including quantum mechanical solute modes is derived in ref. [51].

The free energy surfaces and couplings for PCET reactions may be calculated with a multistate continuum theory.[52] In this theoretical formulation, the PCET free energy surfaces are calculated as functions of two collective solvent coordinates z_p and z_e, corresponding to proton and electron transfer, respectively. For PCET systems in which proton transfer is electronically adiabatic and ET/EPT is electronically nonadiabatic, the reactants (I) are mixtures of the *1a* and *1b* diabatic states, and the products (II) are mixtures of the *2a* and *2b* states. The proton vibrational states are calculated numerically for both the reactant (I) and product (II) ET diabatic surfaces, resulting in two sets of two-dimensional free energy surfaces that are approximate paraboloids, as depicted in Figure 6.

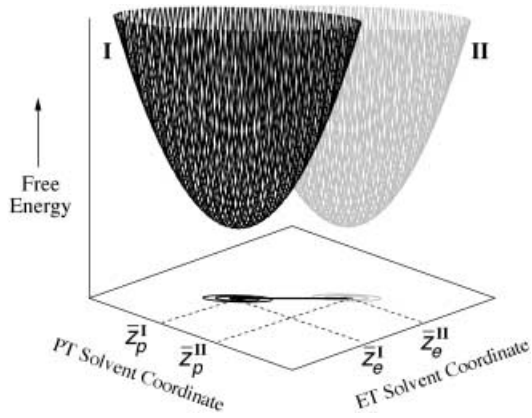

Figure 6. *ET diabatic free energy surfaces as functions of two collective solvent coordinates, z_p and z_e, for PCET between iron biimidazoline complexes. For simplicity, only the lowest free energy surface for each ET state is shown, and the dependence of the free energy surfaces on the inner-sphere coordinates is not included. Data reproduced with permission from ref. [64].*

The mechanism for an electronically nonadiabatic PCET reaction is illustrated in Figure 7. The PCET reaction is described in terms of nonadiabatic transitions from the reactant (I) to the product (II) mixed electronic/vibrational ET diabatic surfaces. Figure 7a depicts a slice of the two-dimensional free energy surfaces for the PCET reaction. This slice connects the minima of the two lowest ET diabatic surfaces shown in Figure 6, so the reaction coordinate is diagonal in the two-dimensional solvent space. Although excited vibrational states play a role, for simplicity only the lowest vibrational states are shown in Figure 7. Figure 7b shows the reactant and product proton potential energy curves (labeled I and II, respectively) and the corresponding proton vibrational wavefunctions as functions of the proton coordinate r_p for select solvent coordinates (z_p,z_e).

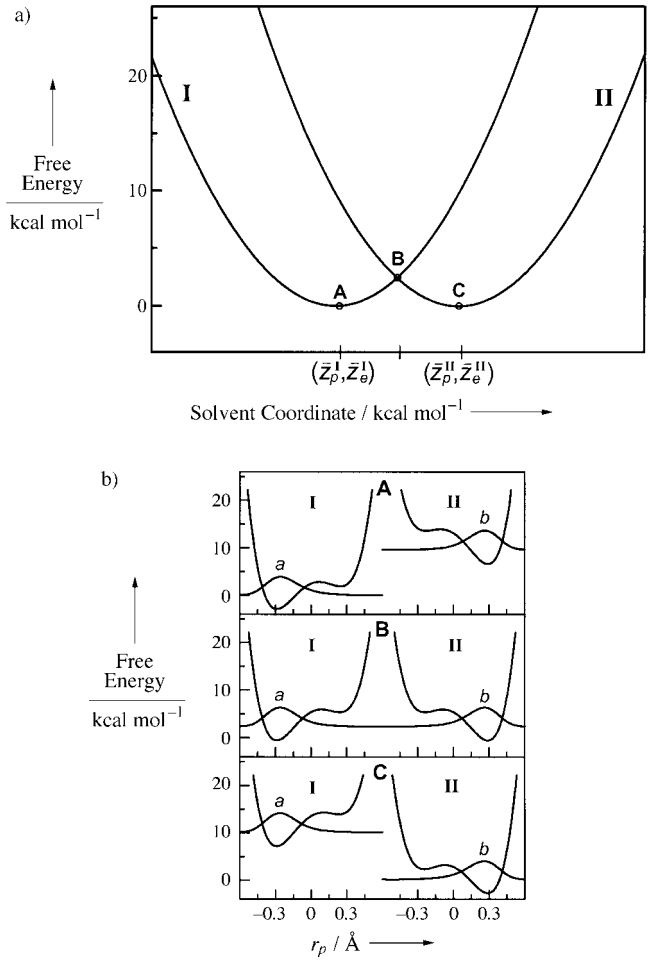

Figure 7. *a) Slice of the two-dimensional ET diabatic free energy surfaces along the line connecting the two minima for PCET between iron biimidazoline complexes. The lowest energy reactant (I) and product (II) free energy surfaces are shown. Points A, B, and C, respectively, represent the equilibrium reactant configuration, the intersection point, and the equilibrium product configuration. b) Proton potential energy curves and corresponding ground-state proton vibrational wavefunctions as functions of the proton coordinate* r_p *for the solvent coordinates associated with points A, B, and C indicated above in (a). The proton potential energy curves are labelled I (or II) to denote the reactant (or product) ET diabatic free energy surface. The proton vibrational wavefunctions are labelled* a *(or* b*) to indicate the dominant PT state. Data reproduced with permission from ref. [64].*

The asymmetry of these proton potential-energy curves is due to the different charges on the electron donor and acceptor on each side of the proton transfer interface. As a result of electrostatic interactions, in the reactant (I) proton potential-energy curve the *a* well is lower in energy, while in the product (II) proton potential energy curve the *b* well is lower in energy. This asymmetry remains along the entire PCET reaction path, regardless of the solvent coordinates. On the other hand, Figure 7 b shows that altering the solvent coordinates along the reaction path influences the relative energies of the reactant and product vibrational states. At the intersection point of the free energy surfaces, the ground vibrational states for the reactant and product are degenerate. The nonadiabatic transition between these two surfaces represents simultaneous quantum mechanical tunneling of a proton and an electron. In addition, this theory also encompasses the description of sequential PCET reactions, in which electron transfer occurs prior to proton transfer or the other way around.[60]

The implementation of this multistate continuum theory requires the following input quantities: the gas-phase solute EVB Hamiltonian matrix elements, the outer-sphere reorganization energy matrix elements, and the inner-sphere reorganization energy. The gas-phase solute matrix elements are represented by standard molecular mechanical terms fit to electronic structure calculations or experimental data. The outer-sphere reorganization energy matrix elements are calculated with an electrostatic model such as the frequency-resolved cavity model (FRCM).[66, 67] The inner-sphere reorganization energy due to the metal – ligand modes may be calculated from a harmonic model based on the calculated or measured frequencies. The effects of the proton donor – acceptor mode may be included by treating this mode quantum mechanically on the same level as the transferring proton. This approach has also been extended to cases in which the electron transfer is coupled to multiple protons.[61]

The methods described in Section 2 for the mixed quantum/classical simulation of proton, hydride, and hydrogen atom transfer reactions in solution or proteins may also be applied to PCET reactions. For PCET, a four-state VB model is required, and the free energy surfaces depend on two collective coordinates corresponding to ET and PT defined analogously to the coordinate given in Equation (4). For electronically nonadiabatic PCET, the relevant free energy surfaces are the two sets of ET diabatic surfaces corresponding to reactants (I) and products (II). These surfaces are obtained by diagonalization of two separate 2×2 EVB Hamiltonian matrices (corresponding to *1a*/*1b* and *2a*/*2b*, respectively). We have calculated these types of two-dimensional free energy surfaces for a model PCET reaction in solution using molecular dynamics methods with explicit solvent molecules.[62] The rates for this PCET reaction have been calculated by the application of the Golden Rule to the two sets of ET diabatic free energy surfaces. Dynamic effects may be included by initiating trajectories near the nonadiabatic crossings of the two sets of ET diabatic free energy surfaces.

3.2. Application

We have applied the multistate continuum theory described above to PCET in iron biimidazoline complexes, as depicted in Scheme 1.[64] These calculations were motivated by experimental studies which show that the rates of electron transfer and PCET are similar and are both slower than the rate of proton transfer for these systems.[68] A previous analysis of this reaction assumed that the electron transfer reaction is electronically adiabatic and viewed the PCET reaction as an electronically adiabatic hydrogen atom transfer reaction.[68] In our theoretical treatment, the electron transfer reaction was assumed to be electronically nonadiabatic. This assumption is based on the following factors. First, the distance between the iron centers in the experimental crystal structure is relatively large, 10.3 Å. In addition, preliminary generalized Mulliken – Hush calculations on these iron biimida-

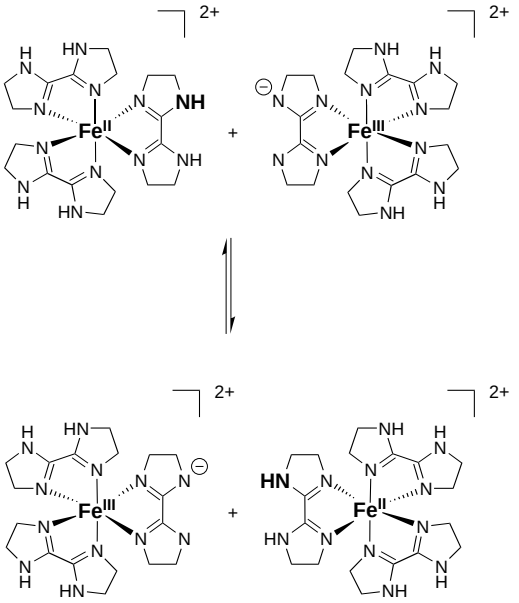

Scheme 1. Proton-coupled electron transfer (PECT) reaction between iron biimidazoline complexes.

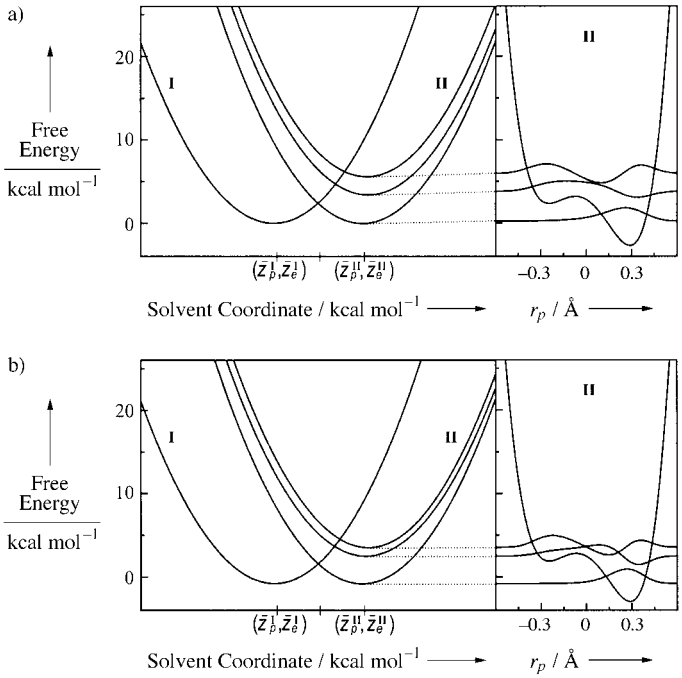

Figure 8. *a) Slice of the two-dimensional ET diabatic free energy surfaces along the line connecting the two minima for PCET between iron biimidazoline complexes with a) hydrogen and b) deuterium. On the left are the free energy surfaces as functions of the solvent coordinates, including the lowest energy reactant (I) and the lowest three product (II) free energy surfaces. On the right are the product (II) proton potential energy curves and the corresponding proton vibrational wavefunctions as functions of the proton coordinate r_p evaluated at the minimum of the ground-state product free energy surface. Note that the energies associated with the proton vibrational wavefunctions coincide with the energies of the product free energy surfaces. Data reproduced with permission from ref. [64].*

zoline complexes suggest that the electronic couplings are in the electronically nonadiabatic regime at 298 K. Another indication that this ET reaction is electronically nonadiabatic is that substitution of the calculated total reorganization energy into the rate expression for electronically adiabatic ET does not reproduce the experimentally determined rate. Furthermore, we calculated a substantial outer-sphere solvent reorganization energy for PCET (approximately 85 % of the solvent reorganization energy for ET). This relatively large outer-sphere reorganization energy indicates a significant change in solute charge distribution during this reaction. The electronic nonadiabaticity and the substantial solvent reorganization for PCET suggest that this is *not* a hydrogen atom transfer reaction as defined in this Minireview, because the electron and proton are not transferred between the same donor and acceptor.

Our calculations accurately reproduced the experimentally measured rates and deuterium kinetic isotope effects for electron transfer and PCET. The lowest energy reactant (I) and product (II) free energy surfaces are given in Figures 6 and 7. The excited product mixed electronic/vibrational free energy surfaces for hydrogen and deuterium are depicted in Figure 8. Our calculations indicate that the similarity of the rates for electron transfer and PCET is due mainly to the compensation of the larger outer-sphere solvent reorganization for electron transfer by the smaller coupling for PCET, which results from the averaging over the reactant and product proton vibrational wavefunctions. Excited vibrational product states were also found to play a role in the PCET reaction. The proton transfer reaction was found to be dominated by solute reorganization (with very small solvent reorganization energy) and to be electronically adiabatic, leading to a fundamentally different mechanism which accounts for the faster rate. This difference is evident by comparing Figure 2, which represents an electronically adiabatic hydrogen transfer reaction, and Figure 7, which represents an electronically nonadiabatic PCET reaction.

The kinetic isotope effect for this iron biimidazoline system is moderate ($k_H/k_D = 2.3$) due to the relatively short distance, between the proton donor and acceptor. A short proton transfer distance leads to a low barrier along the proton coordinate and partially delocalized ground-state proton vibrational wavefunctions, as well as contributions from delocalized excited proton vibrational states. Thus, the ground-state reactant and product proton vibrational wavefunctions overlap significantly, as depicted in Figure 9 a. In our theoretical formulation, the coupling is averaged over the reactant and product vibrational wavefunctions. Assuming the kinetic isotope effect is dominated by differences in this averaged coupling, the kinetic isotope effect is approximately proportional to the square of the ratio of the overlap of the hydrogen reactant and product vibrational wavefunctions and the deuterium reactant and product vibrational wavefunctions. As evident in Figure 9, this ratio becomes larger as the overlap of the reactant and product hydrogen vibrational wavefunctions decreases.

Thus, this theory predicts that the kinetic isotope effect would increase if the proton transfer distance were increased, leading to a higher and wider barrier along the proton coordinate and thus to more separated proton vibrational wavefunctions (Fig-

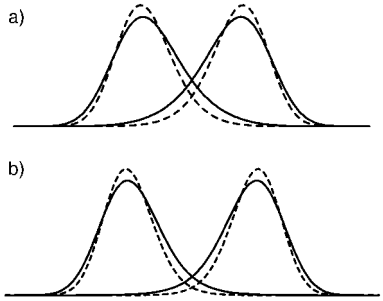

Figure 9. *Reactant and product vibrational wavefunctions as functions of the proton coordinate r_p for H (——) and D (- - - -): a) Short donor – acceptor distance with significant overlap that is similar for H and D, leading to a moderate kinetic isotope effect and b) longer donor – acceptor distance with smaller overlap that differs significantly for H and D, leading to a larger kinetic isotope effect.*

ure 9 b).[60] When the proton transfer distance is increased too much, however, the proton transfer reaction will no longer occur, and the mechanism will be ET rather than PCET. Thus, the maximum kinetic isotope effect is expected to occur for intermediate proton transfer distances. Larger kinetic isotope effects of up to $\sim$40 have been measured experimentally for other PCET reactions, such as oxoruthenium complexes.[69–72] Currently we are applying the multistate continuum theory to these oxoruthenium complexes.

4. Concluding Remarks

This Minireview has presented a theoretical perspective of hydride, hydrogen atom, and PCET reactions. Here hydride and hydrogen atom transfer refer to reactions in which the electrons and protons transfer between the same donors and acceptors, while PCET refers to reactions in which the electrons and protons transfer between different centers. Note that these definitions depend on only the initial and final states and hence do not pertain to the electron – proton coupling during the reaction. Nevertheless, these definitions provide a framework for the analysis of these types of reactions. In particular, these definitions imply that hydride and hydrogen atom transfer reactions are electronically adiabatic, whereas PCET reactions involving the transfer of an electron through a proton transfer interface are typically electronically nonadiabatic. For all three types of reactions, solute reorganization is important, particularly the hydrogen donor – acceptor mode. Hydride transfer and PCET reactions require substantial solute charge redistribution, whereas hydrogen atom transfer reactions do not involve significant charge redistribution. Thus, solvent reorganization is important for hydride transfer and PCET reactions but not for hydrogen atom transfer reactions. In this Minireview, we have presented theoretical descriptions and simulation methodology for all three types of reactions. Applications to hydride transfer in enzymes and PCET in solution have also been described.

Due to their importance throughout chemistry and biology, hydride, hydrogen atom, and proton-coupled electron transfer reactions are being investigated extensively. The precise definition of these reactions, as well as the understanding of their fundamental properties, will aid in the effective communication between theoreticians and experimentalists, which is vital to further progress in this field. Such progress will lead to the elucidation of the mechanisms and the underlying principles for a wide range of chemical and biological processes.

I owe great thanks to Dr. Hélène Decornez and Dr. Salomon Billeter for their important contributions to this work and for creating all of the figures. I am grateful for financial support from NIH grant GM56207 and NSF grant CHE-0096357, as well as an Alfred P. Sloan Foundation Research Fellowship and a Camille Dreyfus Teacher-Scholar Award.

[1] R. J. Cave, M. D. Newton, *Chem. Phys. Lett.* **1996**, *249*, 15.
[2] R. J. Cave, M. D. Newton, *J. Chem. Phys.* **1997**, *106*, 9213.
[3] S. Hammes-Schiffer, J. C. Tully, *J. Chem. Phys.* **1994**, *101*, 4657.
[4] D. Borgis, G. Tarjus, H. Azzouz, *J. Phys. Chem.* **1992**, *96*, 3188.
[5] D. Laria, G. Ciccotti, M. Ferrario, R. Kapral, *J. Chem. Phys.* **1992**, *97*, 378.
[6] D. Borgis, J. T. Hynes, *Chem. Phys.* **1993**, *170*, 315.
[7] J. Mavri, H. J. C. Berendsen, W. F. van Gunsteren, *J. Phys. Chem.* **1993**, *97*, 13469.
[8] A. Staib, D. Borgis, J. T. Hynes, *J. Chem. Phys.* **1995**, *102*, 2487.
[9] K. Ando, J. T. Hynes, *J. Mol. Liq.* **1995**, *64*, 25.
[10] P. Bala, B. Lesyng, J. A. McCammon, *Chem. Phys.* **1994**, *180*, 271.
[11] D. Li, G. A. Voth, *J. Phys. Chem.* **1991**, *95*, 10425.
[12] J. K. Hwang, A. Warshel, *J. Phys. Chem.* **1993**, *97*, 10053.
[13] J. K. Hwang, Z. T. Chu, A. Yadav, A. Warshel, *J. Phys. Chem.* **1991**, *95*, 8445.
[14] J. Lobaugh, G. A. Voth, *Chem. Phys. Lett.* **1992**, *198*, 311.
[15] H. Azzouz, D. Borgis, *J. Chem. Phys.* **1993**, *98*, 7361.
[16] R. Pomès, B. Roux, *Chem. Phys. Lett.* **1995**, *234*, 416.
[17] S. R. Billeter, W. F. van Gunsteren, *Comput. Phys. Commun.* **1997**, *107*, 61.
[18] R. I. Cukier, J. Zhu, *J. Phys. Chem.* **1997**, *101*, 7180.
[19] M. E. Tuckerman, D. Marx, M. L. Klein, M. Parrinello, *Science* **1997**, *275*, 817.
[20] U. Schmitt, G. A. Voth, *J. Chem. Phys.* **1999**, *111*, 9361.
[21] C. Alhambra, J. C. Corchado, M. L. Sanchez, J. Gao, D. G. Truhlar, *J. Am. Chem. Soc.* **2000**, *122*, 8197.
[22] M. Ben-Nun, T. J. Martinez, *J. Phys. Chem. A* **1999**, *103*, 6055.
[23] V. Guallar, V. S. Batista, W. H. Miller, *J. Chem. Phys.* **2000**, *113*, 9510.
[24] Y. R. Mo, J. L. Gao, *J. Phys. Chem. A* **2000**, *104*, 3012.
[25] W. Thompson, J. T. Hynes, *J. Phys. Chem. A* **2001**, *105*, 2582.
[26] A. Warshel, *Computer Modeling of Chemical Reactions in Enzymes and Solutions*, John Wiley and Sons Inc., New York, NY, **1991**.
[27] P. L. Geissler, C. Dellago, D. Chandler, J. Hutter, M. Parrinello, *Science* **2001**, *291*, 2121.
[28] "Proton-Coupled Electron Transfer": S. Hammes-Schiffer in *Electron Transfer in Chemistry, Vol. I* (Ed.: V. Balzani), Wiley-VCH, Weinheim, **2001**.
[29] S. P. Webb, S. Hammes-Schiffer, *J. Chem. Phys.* **2000**, *113*, 5214.
[30] T. Iordanov, S. R. Billeter, S. P. Webb, S. Hammes-Schiffer, *Chem. Phys. Lett.* **2001**, *338*, 389.
[31] R. A. Marcus, *Annu. Rev. Phys. Chem.* **1964**, *15*, 155.
[32] L. D. Zusman, *Chem. Phys.* **1980**, *49*, 295.
[33] A. Warshel, *J. Phys. Chem.* **1982**, *86*, 2218.
[34] D. F. Calef, P. G. Wolynes, *J. Phys. Chem.* **1983**, *87*, 3387.
[35] S. R. Billeter, S. P. Webb, T. Iordanov, P. K. Agarwal, S. Hammes-Schiffer, *J. Chem. Phys.* **2001**, *114*, 6925.
[36] E. Wigner, *Phys. Rev.* **1932**, *40*, 749.
[37] C. H. Bennett, *Algorithms for Chemical Computation*, American Chemical Society, Washington, DC, **1997**.
[38] J. C. Keck, *J. Chem. Phys.* **1960**, *32*, 1035.
[39] J. B. Anderson, *J. Chem. Phys.* **1973**, *58*, 4684.
[40] J. C. Tully, *J. Chem. Phys.* **1990**, *93*, 1061.
[41] S. Hammes-Schiffer, *J. Phys. Chem. A* **1998**, *102*, 10443.
[42] S. Hammes-Schiffer, J. C. Tully, *J. Chem. Phys.* **1995**, *103*, 8528.
[43] S. R. Billeter, S. P. Webb, P. K. Agarwal, T. Iordanov, S. Hammes-Schiffer, *J. Am. Chem. Soc.* **2001**, *123*, 11262.
[44] H. Euklund, B. V. Plapp, J. P. Samama, C. Branden, *J. Biol. Chem.* **1982**, *257*, 14359.
[45] S. Ramaswamy, H. Eklund, B. V. Plapp, *Biochemistry* **1994**, *33*, 5230.

[46] B. J. Bahnson, J. P. Klinman, *Methods Enzymol.* **1995**, *249*, 374.
[47] A. Kohen, J. P. Klinman, *Acc. Chem. Res.* **1998**, *31*, 397.
[48] B. J. Bahnson, D. H. Park, K. Kim, B. V. Plapp, J. P. Klinman, *Biochemistry* **1993**, *32*, 5503.
[49] W. F. van Gunsteren, S. R. Billeter, A. A. Eising, P. H. Hünenberger, P. Krüger, A. E. Mark, W. R. P. Scott, I. G. Tironi, *Biomolecular Simulation: The GROMOS96 Manual and User Guide*, Biomos b.v., Zurich and Groningen, VdF Hochschulverlag, ETH Zurich, Zurich, **1996**.
[50] B. J. Bahnson, T. D. Colby, J. K. Chin, B. M. Goldstein, J. P. Klinman, *Proc. Natl. Acad. Sci. USA* **1997**, *94*, 12797.
[51] A. V. Soudackov, S. Hammes-Schiffer, *J. Chem. Phys.* **2000**, *113*, 2385.
[52] A. V. Soudackov, S. Hammes-Schiffer, *J. Chem. Phys.* **1999**, *111*, 4672.
[53] R. I. Cukier, *J. Phys. Chem.* **1994**, *98*, 2377.
[54] X. G. Zhao, R. I. Cukier, *J. Phys. Chem.* **1995**, *99*, 945.
[55] R. I. Cukier, *J. Phys. Chem.* **1995**, *99*, 16101.
[56] R. I. Cukier, *J. Phys. Chem.* **1996**, *100*, 15428.
[57] R. I. Cukier, D. G. Nocera, *Annu. Rev. Phys. Chem.* **1998**, *49*, 337.
[58] A. V. Soudackov, S. Hammes-Schiffer, *J. Am. Chem. Soc.* **1999**, *121*, 10598.
[59] S. Hammes-Schiffer, *Acc. Chem. Res.* **2001**, *34*, 273.
[60] H. Decornez, S. Hammes-Schiffer, *J. Phys. Chem. A* **2000**, *104*, 9370.
[61] I. Rostov, S. Hammes-Schiffer, *J. Chem. Phys.* **2001**, *115*, 285.
[62] M. Kobrak, S. Hammes-Schiffer, *J. Phys. Chem. B*, **200**, *105*, 10435.
[63] Y. Georgievskii, A. A. Stuchebrukhov, *J. Chem. Phys.* **2000**, *113*, 10438.
[64] N. Iordanova, H. Decornez, S. Hammes-Schiffer, *J. Am. Chem. Soc.* **2001**, *123*, 3723.
[65] R. A. Marcus, N. Sutin, *Biochim. Biophys. Acta* **1985**, *811*, 265.
[66] M. V. Basilevsky, I. V. Rostov, M. D. Newton, *Chem. Phys.* **1998**, *232*, 189.
[67] M. D. Newton, M. V. Basilevsky, I. V. Rostov, *Chem. Phys.* **1998**, *232*, 201.
[68] J. P. Roth, S. Lovel, J. M. Mayer, *J. Am. Chem. Soc.* **2000**, *122*, 5486.
[69] R. A. Binstead, B. A. Moyer, G. J. Samuels, T. J. Meyer, *J. Am. Chem. Soc.* **1981**, *103*, 2897.
[70] R. A. Binstead, L. K. Stultz, T. J. Meyer, *Inorg. Chem.* **1995**, *34*, 546.
[71] B. T. Farrer, H. H. Thorp, *Inorg. Chem.* **1999**, *38*, 2497.
[72] M. H. V. Huynh, T. J. Meyer, P. S. White, *J. Am. Chem. Soc.* **1999**, *121*, 4530.

Received: August 1, 2001 [M274]